

# *Acta Medica Okayama*

---

*Volume 47, Issue 2*

1993

*Article 8*

APRIL 1993

---

## Multivariate analysis of magnetic resonance imaging of focal hepatic lesions.

Mamoru Fujishima\*    Ichizou Suemitsu†    Tetsuro Sei‡  
Yoshihiro Takeda\*\*    Yoshio Hiraki††

\*Okayama University,

†Okayama University,

‡Okayama University,

\*\*Okayama University,

††Okayama University,

# Multivariate analysis of magnetic resonance imaging of focal hepatic lesions.\*

Mamoru Fujishima, Ichizou Suemitsu, Tetsuro Sei, Yoshihiro Takeda, and  
Yoshio Hiraki

## Abstract

A total of 124 lesions from 1 to 6cm in diameter, including 31 cavernous hemangiomas, 32 metastases and 61 hepatocellular carcinomas (HCC) were analyzed to study the usefulness of magnetic resonance imaging (MRI) at 0.5 Tesla to differentiate focal hepatic lesions on the basis of qualitative criteria. Each focal hepatic lesion was assessed for shape, internal architecture and signal intensity relative to normal liver parenchyma. While all cavernous hemangiomas and metastases except one lesion could be detected, detection rate of HCC was significantly inferior to that of the other two diseases. A tumor capsule and a hyperintense focus on T1-weighted images were demonstrated in only HCC lesions in strong contrast with the other two diseases; however, metastases with slow-growing characteristics or subacute hematoma may appear as similar images. Cavernous hemangiomas appeared markedly hyperintense on T2-weighted images in 23 of 31 lesions, but one metastasis and one HCC had similar images. A multivariate analysis of several MRI resulted in the following mean discriminant scores: cavernous hemangioma, -1.2652; metastasis, 0.1830; and HCC, 0.7138. It appeared to be possible to differentiate the three diseases with 84.4 percent accuracy.

**KEYWORDS:** magnetic resonance imaging, liver neoplasms, multivariate analysis

---

\*PMID: 8389524 [PubMed - indexed for MEDLINE]

Copyright (C) OKAYAMA UNIVERSITY MEDICAL SCHOOL

## Multivariate Analysis of Magnetic Resonance Imaging of Focal Hepatic Lesions

Mamoru Fujishima\*, Ichizou Suemitsu, Tetsuro Sei, Yoshihiro Takeda and Yoshio Hiraki

*Department of Radiology, Okayama University Medical School, Okayama 700, Japan*

A total of 124 lesions from 1 to 6cm in diameter, including 31 cavernous hemangiomas, 32 metastases and 61 hepatocellular carcinomas (HCC) were analyzed to study the usefulness of magnetic resonance imaging (MRI) at 0.5 Tesla to differentiate focal hepatic lesions on the basis of qualitative criteria. Each focal hepatic lesion was assessed for shape, internal architecture and signal intensity relative to normal liver parenchyma. While all cavernous hemangiomas and metastases except one lesion could be detected, detection rate of HCC was significantly inferior to that of the other two diseases. A tumor capsule and a hyperintense focus on T<sub>1</sub>-weighted images were demonstrated in only HCC lesions in strong contrast with the other two diseases; however, metastases with slow-growing characteristics or subacute hematoma may appear as similar images. Cavernous hemangiomas appeared markedly hyperintense on T<sub>2</sub>-weighted images in 23 of 31 lesions, but one metastasis and one HCC had similar images. A multivariate analysis of several MRI resulted in the following mean discriminant scores: cavernous hemangioma, -1.2652; metastasis, 0.1830; and HCC, 0.7138. It appeared to be possible to differentiate the three diseases with 84.4 percent accuracy.

*Key words* : magnetic resonance imaging, liver neoplasms, multivariate analysis

The rapid progress of various imaging methods; ultrasonography (US), computed tomography (CT) and magnetic resonance imaging (MRI), has made possible relatively accurate diagnoses of focal hepatic lesions (1-10). Unfortunately equivocal cases continue to challenge the accuracy of these noninvasive techniques.

The purpose of this study was to assess the accuracy of differentiation among hepatocellular carcinoma (HCC), metastasis and cavernous hemangioma by using a multivariate analysis (Hayashi's quantification scaling type II) of several findings observed in MRI.

### Materials and Methods

The MR images of 83 patients with focal hepatic lesions were examined retrospectively at Iwakuni National Hospital and Kousei

Hospital between May 1988 and April 1992. The study included 62 men and 21 women aged 36-83 (mean, 58.0) years old. The 124 lesions evaluated included 31 cavernous hemangiomas in 20 patients, 32 metastases in 16 patients, 61 HCCs in 47 patients. The primary cancers of origin for the metastatic lesions included colorectal (13 lesions), gallbladder (5 lesions), stomach (4 lesions), kidney (3 lesions), pancreas (2 lesions). Five lesions had metastatic adenocarcinoma of unknown origin.

The diagnostic confirmation of individual lesions was made histopathologically in 5 cases and angiographically in 26 cases for cavernous hemangiomas, and histopathologically in all cases for metastases and HCCs.

Tumors smaller than 1 cm in diameter and tumors larger than 6 cm in diameter were excluded, and a maximum of five lesions per patient (the largest lesions) were evaluated.

MR imaging was performed with a superconducting unit (Resona; Yokogawa Medical Systems, Tokyo) operating at 0.5 Tesla. The matrix was 224 × 160. A spin echo (SE) pulse sequence was employed, with a repetition time (TR) of 450-760 msec and an echo time (TE) of 15-21 msec with four excitations (TR/TE = 450-760/15-21) for T<sub>1</sub>-weighted images and SE 1700

\* To whom correspondence should be addressed.

-2050/80-100 with two excitations for T<sub>2</sub>-weighted images. Multiple simultaneous sections were obtained in the transaxial plane in all patients. The section thickness was 10mm, with 2mm intersection gaps.

Each focal hepatic lesion was assessed for shape, internal architecture and signal intensity relative to normal liver parenchyma on T<sub>1</sub>-weighted and T<sub>2</sub>-weighted images on the basis of visual inspection. Shape was designated as smooth or irregular (6). A tumor capsule was demonstrated as a thin circumferential rim, hypointense relative to adjunct liver on T<sub>1</sub>-weighted images (8).

In comparison with the normal liver parenchyma on the T<sub>2</sub>-weighted images, a peritumor halo sign appeared as thick and hyperintense circumferential rim. In contrast to the halo sign, a target sign appeared as markedly hyperintense central zone of the tumor. Lesions were classified as homogeneous when they were of uniform signal intensity throughout (3). In addition, lesions were classified as markedly hyperintense on T<sub>2</sub>-weighted images if they had signal intensities equal to or greater than that of bile within the gallbladder or that of cerebrospinal fluid (3).

MR images obtained at soft-tissue windows and levels were independently reviewed by two of the authors (M. F., I. S.). All interpretations were made without knowledge of the histologic type of the lesions. When the interpretations differed, a consensus was achieved after both interpreters had reviewed the images together.

Initially, each factor was evaluated for its value in differentiating three diseases on a univariate basis by means of the  $\chi$ -square analysis.

We conducted the evaluation of a multivariate analysis with several variables from the univariate analysis by means of statistical software HALBAU (High-quality Analysis Library for Business and Academic Users).

In this multivariate analysis, the three types of diseases are defined as criterion variables and the factors used for the analysis such as lesion shape, internal architecture, and signal intensity characteristics are defined as explanatory variables.

## Results

The contingency table between each factor and the diseases is shown in Table 1. When any frequency in the table was 5 or less, Fisher's test was adopted. The distribution of the size was not statistically significant in the three diseases. Except one metastatic lesion, all cavernous hemangiomas and metastases larger than 1 cm were detectable under the already described condition. However, HCC could not be imaged with statistical significance by the  $\chi$ -square analysis at a 0.01 level. The metastases were irregular in shape, but irregular shape did not occur in the other two diseases with statistical significance by the  $\chi$ -square analysis at a 0.01 level. A tumor capsule was demonstrated in HCC, but not in the

other two diseases. Halo or target signs appeared in metastases frequently, and they could be observed in 3.3 percent of HCCs. Metastases appeared homogeneously hypointense on T<sub>1</sub>-weighted images significantly compared with HCCs. Cavernous hemangiomas and metastases never showed a hyperintense focus on T<sub>1</sub>-weighted

**Table 1** Correlation between various factors and three different hepatic lesions

Factor	Number of lesions		
	Cavernous hemangioma (n = 31)	Metastasis (n = 32)	Hepatocellular carcinoma (n = 61)
Size <sup>a</sup> (cm)			
1 ~ 2	11	11	19
2.1 ~ 4	15	16	35
4.1 ~ 6	5	5	7
Can be imaged by MRI			
Yes	31	31	47
No	0	1	14
		* **	
Shape <sup>b</sup>			
Smooth	10	2	19
Irregular	21	29	28
	* *		*
Tumor capsule <sup>c</sup>			
No	31	31	26
Yes	0	0	21
			*
Halo/Target sign <sup>d</sup>			
No	31	20	59
Yes	0	12	2
	* *		*
Homogeneously hypointense on T <sub>1</sub> -weighted images			
Yes	21	28	6
No	10	4	55
			*
Hyperintense focus on T <sub>1</sub> -weighted images			
No	31	32	36
Yes	0	0	25
			*
Markedly hyperintense on T <sub>2</sub> -weighted images			
Yes	23	1	1
No	8	31	60
	* *		*

a: The major axis was measured. b: The cases undetectable on T<sub>1</sub>-weighted images or on T<sub>2</sub>-weighted images were excluded. c: The presence of tumor capsule was estimated on T<sub>1</sub>-weighted images and undetectable cases were excluded. d: The presence of halo or target sign was estimated on T<sub>2</sub>-weighted images. Statistical significance was determined by  $\chi$ -square test or Fisher's test. \*: p < 0.01; \*\*: p < 0.05.

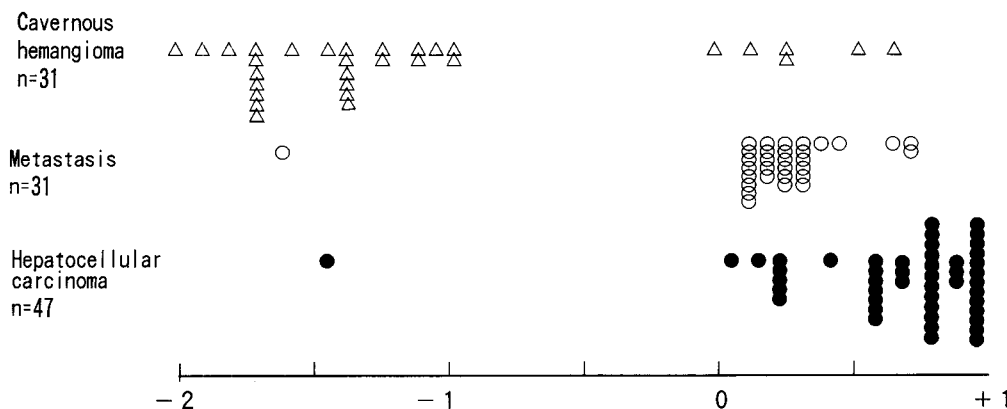


Fig. 1 Scatter plot of discriminant score for cavernous hemangioma, metastasis and hepatocellular carcinoma

images, in strong contrast with HCCs. Cavernous hemangiomas appeared markedly hyperintense on  $T_2$ -weighted images in 23 of 31 lesions; however, one metastasis and one HCC showed the similar images. Further analysis was undertaken by selecting several combinations of MRI findings in order to determine their feasibility for clinical diagnosis. The explanatory variables included in the Hayashi's quantification scaling type II were as follows; size, shape, whether it was homogeneously hypointense on  $T_1$ -weighted images or not, and whether it was markedly hyperintense on  $T_2$ -weighted images. Because other factors had a frequency zero in the  $\chi$ -square table, they could not be used. The discriminant score is expressed by the sum of the four corresponding discriminant coefficients. The discriminant coefficients are determined to maximize the distance of the mean discriminant scores of each criterion variable. All the discriminant scores are shown in Fig. 1. Each case was diagnosed as the disease for which the mean discriminant score was most approximate to the calculated discriminant score. The agreement rate of the real disease to the diagnosis obtained by means of this analysis, or the discrimination success rate was 84.4 percent, while the rates for cavernous hemangioma, metastasis and HCC were 80.6, 87.5 and 88.5 percent, respectively.

## Discussion

Recent articles have described the usefulness of hepatic MRI for distinguishing cavernous hemangiomas from metastases (1, 2, 6, 9) or cavernous hemangiomas

from HCCs (5) either on the basis of visual appearance (2, 6) or by the use of  $T_1$  and  $T_2$  values (1, 2, 5, 6). However, there was significant overlap among the three diseases even when qualitative and quantitative criteria were used. For example, a typical cavernous hemangioma shows as markedly hyperintense on  $T_2$ -weighted images (11). Nevertheless, it is generally known that the characteristic appearance of cavernous hemangiomas includes hypervascular endocrine tumors, sarcomas, uterine carcinoma (2), pancreatic adenocarcinoma (6) *etc.* In this study, no significant difference was shown between the hypervascular tumor and hypovascular one. Moreover, one metastasis and one HCC had these typical images, and consequently it is difficult to differentiate them completely by looking only at MRI findings (11, 12). However, cavernous hemangiomas larger than 1 cm show as hyperintense, sometimes markedly, on  $T_2$ -weighted images, and it is thought that MRI is suitable for detecting them (11, 13-15). On the other hand, the detection rate of HCC is significantly inferior to that of the other two diseases. Accordingly, even if a lesion is revealed by means of US or CT and it is impossible to detect by MRI, it should be emphasized that it can be HCC.

Irregular-shaped lesions exist more often in metastases than in the other two diseases. This information is useful for distinguishing them except large cavernous hemangiomas. Because in the case of large cavernous hemangioma, tumors may undergo thrombosis and form central scars, causing them to have lobulated contours and a nonhomogenous internal signal intensity (14, 16, 17).

Though halo or target signs are said to be specific to metastases (9), in this study a halo sign was also seen in

HCC. This suggests that it is necessary to differentiate them with reference to laboratory data, past history and ultrasonographic or CT findings.

In this study the presence of a hyperintense focus on T<sub>1</sub>-weighted images was characteristic to HCC. It should be noted that metastasis with subacute hematoma may also present the same kind of image. Although the presence of a tumor capsule in an HCC lesion seems to result in a specific finding in MRI (4, 8, 14), slow-growing metastasis may also have a capsular structure.

We encountered several equivocal cases when we focused on singular MRI findings. However, by using a multivariate analysis of several MRI findings, we were able to differentiate the three diseases with more than an 80-percent accuracy which would obviate angiography or biopsy for cavernous hemangiomas detected by noninvasive diagnostic methods.

It was believed that Hayashi's quantification scaling type II should be applied to a clinical study like this one. However, in an HCC lesion, the shape, internal architecture and signal intensity of the tumor may change as tumor size increases. It was, therefore, concluded that more cases should be studied, and in order to improve the accuracy of the diagnoses, the criterion variables should be more strictly selected.

**Acknowledgment.** The authors thank Drs. Takeo Ohta, Toshihide Tsuda and Takanori Ogawa who have helped in this study.

## References

1. Itoh K, Saini S, Hahn PF, Imam N and Ferrucci JT: Differentiation between small hepatic hemangiomas and metastases on MR images: Importance of size-specific quantitative criteria. *Am J Radiol* (1990) **155**, 61-66.
2. Lombardo DM, Baker ME, Spritzer CE, Blinder R, Meyers W, Herfkens RJ: Hepatic hemangiomas vs metastases: MR differentiation at 1.5T. *Am J Radiol* (1990) **155**, 55-59.
3. Brown JJ, Lee JM, Lee JKT, Van Lom KJ and Malchow SC: Focal hepatic lesions: Differentiation with MR imaging at 0.5T. *Radiology* (1991) **179**, 675-679.
4. Itoh K, Nishimura K, Togashi K, Fujisawa I, Noma S, Minami S, Sagoh T, Nakano Y, Itoh H, Mori K, Ozawa K and Torizuka K: Hepatocellular carcinoma: MR imaging. *Radiology* (1987) **164**, 21-25.
5. Ohtomo K, Itai Y, Yoshikawa K, Kokubo T and Iio M: Hepatocellular carcinoma and cavernous hemangioma: Differentiation with MR imaging. *Radiology* (1988) **168**, 621-623.
6. Li KC, Glazer GM, Quint LE, Francis IR, Aisen AM, Ensminger WD and Bookstein FL: Distinction of hepatic cavernous hemangioma from hepatic metastases with MR imaging. *Radiology* (1988) **169**, 409-415.
7. Rummeny E, Weissleder R, Stark DD, Saini S, Compton CC, Bennett W, Hahn PF, Wittenberg J, Malt RA and Ferrucci JT: Primary liver tumors: Diagnosis by MR imaging. *Am J Radiol* (1989) **152**, 63-72.
8. Ebara M, Ohto M, Watanabe Y, Kimura K, Saisho H, Tsuchiya Y, Okuda K, Arimizu N, Kondo F, Ikehira H, Fukuda N and Tateno Y: Diagnosis of small hepatocellular carcinoma: Correlation of MR imaging and tumor histologic studies. *Radiology* (1986) **159**, 371-377.
9. Wittenberg J, Stark DD, Forman BH, Hahn PF, Saini S, Weissleder R, Rummeny E and Ferrucci JT: Differentiation of hepatic metastases from hepatic hemangiomas and cysts by using MR imaging. *Am J Radiol* (1988) **151**, 79-84.
10. Stark DD, Felder RC, Wittenberg J, Saini S, Butch RJ, White ME, Edelman RR, Mueller PR, Simeone JF, Cohen AM, Brady TJ and Ferrucci JT: Magnetic resonance imaging of cavernous hemangioma of the liver: Tissue-specific characterization. *Am J Radiol* (1985) **145**, 213-222.
11. Glazer GM, Aisen AM, Francis IR, Gyves JW, Lande I and Adler DD: Hepatic cavernous hemangioma: Magnetic resonance imaging. *Radiology* (1985) **155**, 417-420.
12. Ohtomo K, Itai Y, Matsuoka Y, Minami M, Okada Y, Kawauchi N, Iio M, Nagashima I and Shiga J: Hepatocellular carcinoma: MR appearance mimicking cavernous hemangioma. *J Comput Assist Tomogr* (1990) **14**, 650-652.
13. Itai Y, Ohtomo K, Furui S, Yamauchi T, Minami M and Yashiro N: Noninvasive diagnosis of small cavernous hemangioma of the liver: Advantage of MRI. *Am J Radiol* (1985) **145**, 1195-1199.
14. Ohtomo K and Itai Y: Magnetic resonance imaging of liver neoplasms. *Jpn J Clin Oncol* (1990) **20**, 21-29.
15. Itai Y, Ohnishi S, Ohtomo K, Kokubo T, Imawari M and Atomi Y: Hepatic cavernous hemangioma in patients at high risk for liver cancer. *Acta Radiol* (1987) **28**, 697-701.
16. Rummeny E, Saini S, Wittenberg J, Compton C, Hahn PF, Mueller PR, Simeone JF, Stark DD, Weissleder R, Dousset MG and Ferrucci JT: MR imaging of liver neoplasms. *Am J Radiol* (1989) **152**, 493-499.
17. Ros PR, Lubbers PR, Olmsted WW and Morillo G: Hemangioma of the liver: Heterogeneous appearance on T<sub>2</sub>-weighted images. *Am J Radiol* (1987) **149**, 1167-1170.

Received September 3, 1992; accepted November 24, 1992.